

# Physical Properties of Compounds Promoting Oral Delivery of Macromolecular Drugs

RUEL Z. B. DESAMERO,<sup>1</sup> HU CHENG,<sup>1</sup> SEAN CAHILL,<sup>2</sup> MARK GIRVIN,<sup>2</sup> HUA DENG,<sup>2</sup> ROBERT CALLENDER,<sup>2</sup> PARSHURAM RATH,<sup>3</sup> BRUCE VARIANO,<sup>3</sup> JOHN E. SMART<sup>3</sup>

<sup>1</sup> Department of Physics, City College of New York, New York, New York 10031

<sup>2</sup> Department of Biochemistry, Albert Einstein College of Medicine, Bronx, New York 10461

<sup>3</sup> Emisphere Technologies, Inc., 756 Old Saw Mill River Road, Tarrytown, New York 10591

Received 17 May 2001; revised 10 August 2001; accepted 4 September 2001

**ABSTRACT:** The spectroscopic and solution properties of a series of amidated acids (delivery agents), which promote the gastrointestinal absorption of USP heparin and other drugs that show poor oral bioavailability, are investigated using Raman and NMR spectroscopy. The results show evidence for self-association at low concentrations of delivery agents that increases as the concentration of the delivery agent is increased. The self-associate is characterized by ring–ring stacking interactions, and the best geometrical arrangement for the stacking is the parallel-shifted arrangement of the rings. In addition, the amide group participates in the formation of intermolecular hydrogen bonds in the self-associate. Unlike the rigid ring, the tails of these delivery agents remain relatively flexible in the self-associate. It is suggested that the limited solubility of the delivery agents at physiological pH arises from a percentage of protonated carboxyls. Their presence promotes the formation of intermolecular hydrophobic and ring stacking interactions, which are otherwise weakened by an ionized carboxyl group. © 2002 John Wiley & Sons, Inc. *Biopolymers (Biospectroscopy)* 67: 26–40, 2002; DOI 10.1002/bip.10039

**Keywords:** physical properties; oral delivery; macromolecular drugs; amidated acids

## INTRODUCTION

The oral bioavailability of macromolecular drugs like heparin and protein drugs is plagued with problems. These molecules are usually unstable in the intestinal environment, because they are susceptible to acid hydrolysis, enzymatic degradation, and bacterial fermentation, which prevents their effective delivery.<sup>1,2</sup> Moreover, be-

cause of the size, charge, and/or hydrophilicity of these macromolecular drugs, transport through the intestinal epithelium is poor.<sup>3</sup> Thus, these drugs can only be effectively administered parenterally at present. However, intravenous delivery or subcutaneous injections have substantial disadvantages and the attractiveness of orally delivered macromolecular drugs is clear.<sup>4,5</sup> Leone-Bay et al. reported the discovery of a series of amidated acids that promote the gastrointestinal absorption of salmon calcitonin,<sup>1</sup> interferon- $\alpha$ ,<sup>1</sup> recombinant human growth hormone,<sup>2</sup> and USP heparin<sup>6–9</sup> in rats and primates. These drug delivery agents elicit no unwanted pharmacological effects, and the increased drug transit across the intestinal membranes is not a result of mucosal

Correspondence to: R. Callender (call@aecom.yu.edu).

Contract grant sponsor: Institute of General Medicine, National Institutes of Health; contract grant number: GM35183.

Contract grant sponsor: Emisphere Technologies, Inc.

*Biopolymers (Biospectroscopy)*, Vol. 67, 26–40 (2002)  
© 2002 John Wiley & Sons, Inc.

damage.<sup>1,2,10-12</sup> Although these drug delivery agents have been shown to enhance drug absorption, the mechanism by which this occurs has not been elucidated.<sup>1,2,6-8</sup> A description of the interactions these delivery agents make with one another and/or with the macromolecular drugs is an essential step toward achieving the goal of understanding the mechanism of action of these drug delivery agents.

The use of Raman vibrational spectroscopy to study the structures of molecules and their interaction with biomacromolecules is well documented.<sup>13-19</sup> The present work takes advantage of the volumes of Raman measurements already taken on simple molecules<sup>20-24</sup> to help identify the major bands in the Raman spectra of the drug delivery agents. Analyses of the vibrational band assignments reveal the structural attributes of these delivery agents in solution. Marker bands that are characteristic of complex formation are identified and used to analyze the structures of self-associated complexes. In addition, Raman difference spectroscopy is used to study the structures of the drug delivery compounds. For complicated systems, like drug delivery agents that self-associate and/or associate with drugs, the vibrational spectrum is hampered by spectral crowding.<sup>17-19</sup> Many vibrational modes contribute to the spectrum of a complex molecular system at each frequency, which results in a spectrum that is very difficult to interpret. In the current studies the spectra of the complex formed between drug delivery agents, as well as the unassociated agent, are taken. Subtraction of the latter from the former to form the difference spectrum should yield the spectrum of those modes affected by the self-association. Raman difference spectroscopy has been successfully used to elucidate the mechanism of enzyme action,<sup>25-29</sup> to determine the secondary structure in proteins,<sup>30,31</sup> and to estimate the extent of hydrogen bonding.<sup>32-34</sup> The subsequent article in this two part study concerns itself with the characterization of the interactions of the drug delivery compounds with heparin.<sup>35</sup>

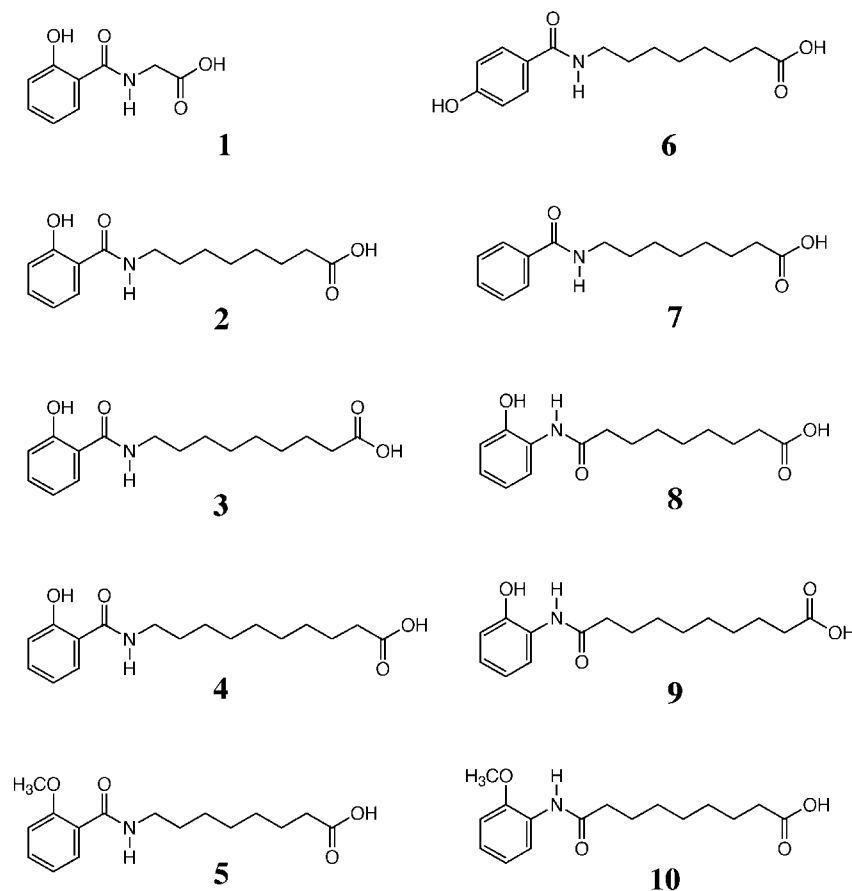
NMR spectroscopy is also employed in our study of the solution structures of the delivery agents and their self-associated complexes. Standard proton NMR measurements were performed on several delivery agents to qualitatively determine the concentration dependence of the NH hydrogen exchange rate and the tumbling rates of different parts of the molecules. It was found that as the concentration of the delivery agents is sig-

nificantly increased, the NH hydrogen exchange rate is slowed. The concentration-dependent decrease of the tumbling rate is more obvious near the aromatic ring than in the aliphatic chain portion of the delivery agents. These results are consistent with the conclusions derived from the Raman studies.

## MATERIALS AND METHODS

The synthesis of the amidated acids (compounds **1-12**, Scheme 1) is described elsewhere.<sup>8</sup> All the samples for Raman measurement were dissolved in 15 mM phosphate buffer (pH 7.4), 15 mM pyrophosphate buffer (pH 10), or 15 mM *N*-tris-[hydroxymethyl]methyl-3-aminopropane sulfonic acid (TAPS) buffer (pH 8.0), depending on the required experimental condition. Once dissolved in the buffer, the pH of the solution was adjusted to the desired value by the gradual addition of either 1*N* sodium hydroxide (NaOH) or hydrochloric acid (HCl) solution. In some cases, to help ascertain the vibrational modes responsible for a few of the characteristic Raman peaks, the compounds were dissolved in a buffered deuterium oxide (D<sub>2</sub>O) solution. In the Raman difference studies each side of a specially fabricated split cell cuvette (Hellma Cells, Jamaica, NY) was loaded with about 30  $\mu$ L of the samples whose difference spectrum was to be determined. The cuvette, which was mounted on a translator stage-stepping motor combination device (Unidex XI with ATS302 stages, Aerotech Inc., Pittsburgh, PA), can be automatically moved side to side (or from cell to cell) without variation in the optical alignment of the setup. This allows for the sequential and repetitive determination of the parent spectra making up the difference spectrum.<sup>17-19</sup>

To induce Raman scattering the sample was irradiated with about 100 mW of a 530.9- or 568.2-nm line of a Coherent Innova 400-K3-krypton ion laser (Coherent Radiation Inc., Palo Alto, CA). Situated 90° from the incident beam was the detection system consisting primarily of an 1877-0.6 m Triplemate spectrometer (Spex Industries, Metuchen, NJ) and a LN/CCD-1152UV detector with a ST-133 controller (Princeton Instruments, Princeton, NJ). The whole optical multichannel analyzer system was interfaced with a Mac IIfx computer (Apple, Cupertino, CA), which made use of the program Igor (WaveMetrics, Lake Oswego, OR) for data collection and analyses. All spectra were corrected for the nonuniform spec-



**Scheme 1.** The structures of the amidated acids in the study.

tral response of the detector and calibrated against the known Raman lines of toluene. The spectrometer slits were set to achieve a spectral resolution of  $6\text{ cm}^{-1}$ . The reproducibility in the band position measurements was  $\pm 1\text{ cm}^{-1}$ . The solvent background Raman spectrum was subtracted from the presented data and none of the data were smoothed. All Raman measurements were done at room temperature, and delivery agent concentrations ranged from 5 to 150 mg/mL.

The NMR measurements were performed on a Bruker DRX-300 spectrometer at  $27^\circ\text{C}$ . The 1-dimensional (1-D) spectra of compounds **2** and **10** were obtained on samples dissolved in 90%  $\text{H}_2\text{O}$ /10%  $\text{D}_2\text{O}$  with 50 mM phosphate buffer (pH 7.4). The solvent peak was suppressed using the Watergate technique.<sup>36</sup> The 1-D selective nuclear Overhauser effect spectroscopy (NOESY) spectra of compound **4** in  $\text{D}_2\text{O}$  at pH 8 were obtained by the double pulsed field gradients spin echo pulse sequence with a mixing time of 400 ms.<sup>37</sup> The

selective pulse has a Gaussian line shape, and the strength of the pulse was set to 10 Hz.

## RESULTS

### Variations in Raman Spectra

Figure 1 shows the Raman spectra of 10 mg/mL solutions of the compounds in the study (Scheme 1). All solutions were at a pH of 7.4, except for compounds **3**, **4**, and **9** where the pH of the solution was adjusted to around 8.0 because of poor solubility. Subtle differences in the structure of the compounds under study (Scheme 1) leads to corresponding variations in the resulting Raman spectra. The structures of compounds **1**, **2**, **3**, and **4** differ only in the length of the aliphatic chain separating the amide moiety from the carboxyl tail of the molecules. The same is true for compounds **8** and **9** (Scheme 1). A comparison of the Raman spectra of these compounds reveals that

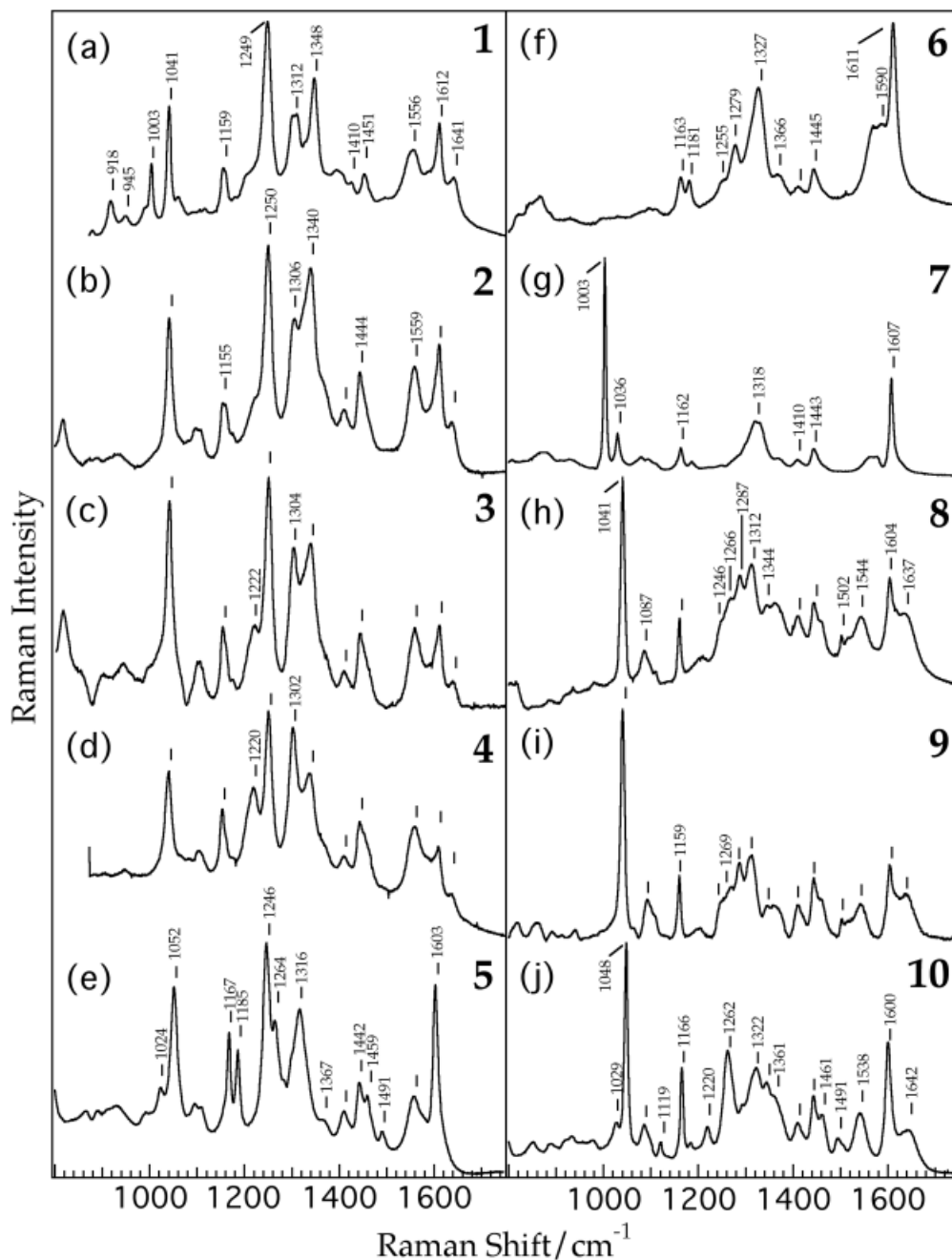


**Figure 1.** Raman spectra of a 10 mg/mL solution of compounds **1** (spectrum a), **2** (spectrum b), **3** (spectrum c), **4** (spectrum d), **5** (spectrum e), **6** (spectrum f), **7** (spectrum g), **8** (spectrum h), **9** (spectrum i), and **10** (spectrum j). All compounds were dissolved in pH 7.4 buffered aqueous solution except for compounds **3**, **4**, and **9** where the pH of the solution had to be adjusted to around 8.0 because of problems with solubility. The Raman bands that shift by less than  $2\text{ cm}^{-1}$  relative to the spectra above it are marked but not labeled.

the difference in the aliphatic chain length does not cause major shifts in the major Raman bands (Fig. 1), although there are many differences in

some of the minor bands. It should be noted that the spectra of compound **1** show a number of peaks in the  $900\text{--}1000\text{ cm}^{-1}$  region that are ab-

sent in the other members of its series (i.e., compounds **2**, **3**, and **4**). This may be due to compound **1** having the shortest aliphatic chain; only one carbon separates the amide moiety from the carboxylic end of the molecule (Scheme 1). The results of this series show that the major bands observed are not likely to originate from the vibrational modes associated with the aliphatic chain.

Reversing the C—N bond orientation of the amide group in the structure of the compound leads to a downshift in the peaks at about 1560 and about 1640  $\text{cm}^{-1}$ , as observed by a comparison of the Raman spectra and the structures of compounds **1–4** to those of compounds **8** and **9** (Scheme 1 and Fig. 1). The 1560  $\text{cm}^{-1}$  band is downshifted by as much as 10  $\text{cm}^{-1}$  while the 1640  $\text{cm}^{-1}$  band downshifts by 3–4  $\text{cm}^{-1}$ . Changing the ring-hydroxy group to a ring-methoxy group (compare compounds **1–4** to compound **5** and compounds **8** and **9** to **10**) also leads to a decrease in the intensity of the band at about 1640  $\text{cm}^{-1}$ . In fact in the Raman spectra of compound **5** (Fig. 1, spectrum e), the band seems to vanish completely or is masked by a peak at about 1600  $\text{cm}^{-1}$ . This indicates that the about 1640  $\text{cm}^{-1}$  Raman band may be associated with a vibrational mode that originates from the amide group of the compounds. Indeed, earlier studies on trans N-monosubstituted amides<sup>22–24</sup> have placed the amide I (or C=O) stretch mode in the 1630–1680  $\text{cm}^{-1}$  region and the amide II in the 1510–1550  $\text{cm}^{-1}$  region. The amide II and amide III (1248–1300  $\text{cm}^{-1}$ ) bands arise from a strong coupling of the C—N—H in-plane deformation and the C—N stretching modes. Amides II and III are both sensitive to deuteration on the amino nitrogen atom and the presence of hydrogen bonding.<sup>22,23</sup> For reasons of band assignments, the Raman spectra of many of these compounds were taken in  $\text{D}_2\text{O}$  (Fig. 2), thereby deutering the amide protons.

Another consequence of reversing the amide orientation is the substantial decrease in the intensity of the bands in the frequency range of 1200–1300  $\text{cm}^{-1}$  relative to the band at about 1040  $\text{cm}^{-1}$  (the peak least affected by changes in the experimental conditions, see below). The band at about 1250  $\text{cm}^{-1}$  is also upshifted by about 16  $\text{cm}^{-1}$  (Fig. 1) when the amide group is attached to the ring via the amide nitrogen instead of the carbonyl carbon (Scheme 1). Although this band falls in the region where the amide III is expected, the assignment is not made because the about

1250  $\text{cm}^{-1}$  band, unlike the about 1560 and 1640  $\text{cm}^{-1}$  bands, is not affected when the compounds are dissolved in  $\text{D}_2\text{O}$ . It is apparent from the Raman spectra of compounds **1**, **2**, **4**, and **8** dissolved in  $\text{D}_2\text{O}$  that the band at about 1640  $\text{cm}^{-1}$  is downshifted to about 1630  $\text{cm}^{-1}$  (Fig. 2). Also evident is the decrease in the intensity of the band at about 1560  $\text{cm}^{-1}$ , as well as the appearance of two new peaks. These new bands, a weak band near 965  $\text{cm}^{-1}$  and an intense peak around 1470  $\text{cm}^{-1}$  for compounds **1**, **2**, and **4**, can be attributed to the N—D bending and C—N stretching modes, respectively.<sup>22–24,38</sup> Upon deuterium exchange of the amide hydrogen, the N—D bending motion is largely decoupled from the C—N stretch due to the much lower N—D bending frequency, and this accounts for the two new peaks. The about 1250  $\text{cm}^{-1}$  band is shifted by no more than 2  $\text{cm}^{-1}$  upon deuteration (Figs. 1 and 2).

The band at about 1250  $\text{cm}^{-1}$  loses intensity when the hydroxyl group in the ring is shifted to the para position (compound **6**). Absence of the 1250  $\text{cm}^{-1}$  band is noted when there is no hydroxy group on the ring (compound **7**). The Raman band at about 1250  $\text{cm}^{-1}$  is also observed to shift in frequency and change in relative intensity when the hydroxy group in the ring moiety of the compound is replaced with a methoxy group (Scheme 1 and Fig. 1). The spectra of compound **5** show two peaks in the area, one at 1246  $\text{cm}^{-1}$  and another at 1264  $\text{cm}^{-1}$ . The relative intensity of the 1246  $\text{cm}^{-1}$  band (but not the 1264  $\text{cm}^{-1}$  one) is comparable to that of the about 1250  $\text{cm}^{-1}$  band in the Raman spectra of compounds **1–4** (Fig. 1). In the spectra of compound **10** the band is upshifted to 1262  $\text{cm}^{-1}$  and is much more intense than the about 1250  $\text{cm}^{-1}$  band in the Raman spectra of compounds **8** and **9**. These results indicate that the about 1250  $\text{cm}^{-1}$  band is very sensitive to changes in the moiety surrounding the aryl-O group. Assigning the about 1250  $\text{cm}^{-1}$  band to the aryl-O stretch is consistent with results already published on phenolic compounds.<sup>21–23,39</sup> Evans<sup>21</sup> concluded from his studies on the difference between the vibrational spectra of phenol and phenol-OD that the aryl-O stretch at about 1250  $\text{cm}^{-1}$  is not sensitive to deuteration.

Always present in the solution Raman spectra of the compounds is the band at 1410  $\text{cm}^{-1}$  (Figs. 1 and 3). However, this band is absent from the spectra of the precipitate form and is replaced by several new bands, most notable of which are the peak at 1730  $\text{cm}^{-1}$  for compound **2** [Fig. 3(a)] or the one at 1715  $\text{cm}^{-1}$  for compound **10** [Fig. 3(b)].

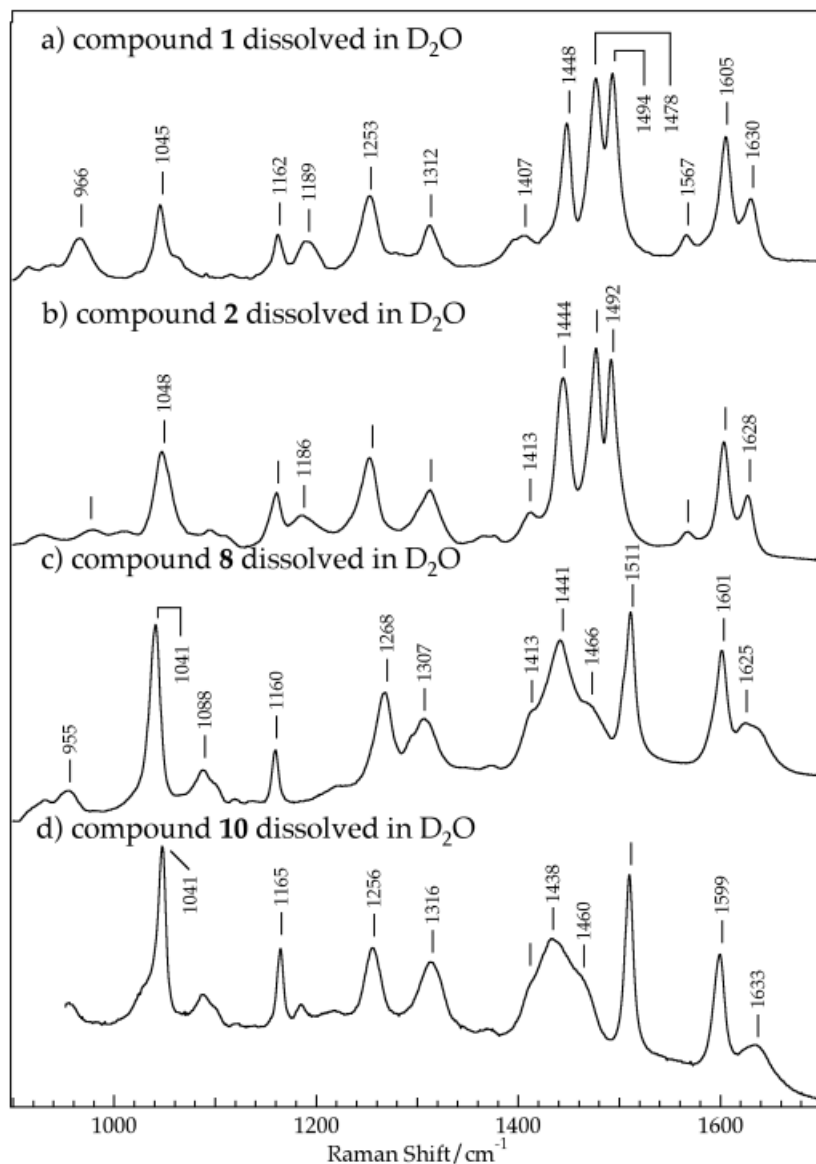


**Figure 2.** Raman spectra of a 10 mg/mL solution of compounds **1** (spectrum a), **2** (spectrum b), **4** (spectrum c), and **8** (spectrum d) dissolved in a buffered (pD 7.4) D<sub>2</sub>O solution. The Raman bands that shift by less than 2 cm<sup>-1</sup> relative to the spectra above it are marked but not labeled.

Similar observations can be noted from a comparison of the precipitate (data not shown) and solution Raman spectra of compounds **1**, **4**, and **8**. Previous studies identified the band at about 1410 cm<sup>-1</sup> as arising from the C=O stretch of an ionized carboxylic group (—COO<sup>-</sup>) whereas the about 1720 cm<sup>-1</sup> band was associated with the protonated —COOH group.<sup>20,22,23</sup> Studies comparing the intensity of the 1410 cm<sup>-1</sup> band to bands observed for ionized acetic acid showed that the 1410 cm<sup>-1</sup> band has the correct intensity

of an ionized carboxyl group (data not shown). Raman measurements using polarized light showed that the 1410 cm<sup>-1</sup> band in acetic acid has the same depolarization ratio as the 1410 cm<sup>-1</sup> band of the compounds. These results show that the carboxylic moiety of the drug delivery agents at 10 mg/mL is in the ionized form in the measured solution (pH 7.4).

Increasing the pH of the solution to 10 brings about changes in the peak intensities and position but no new peaks were added or deleted from the

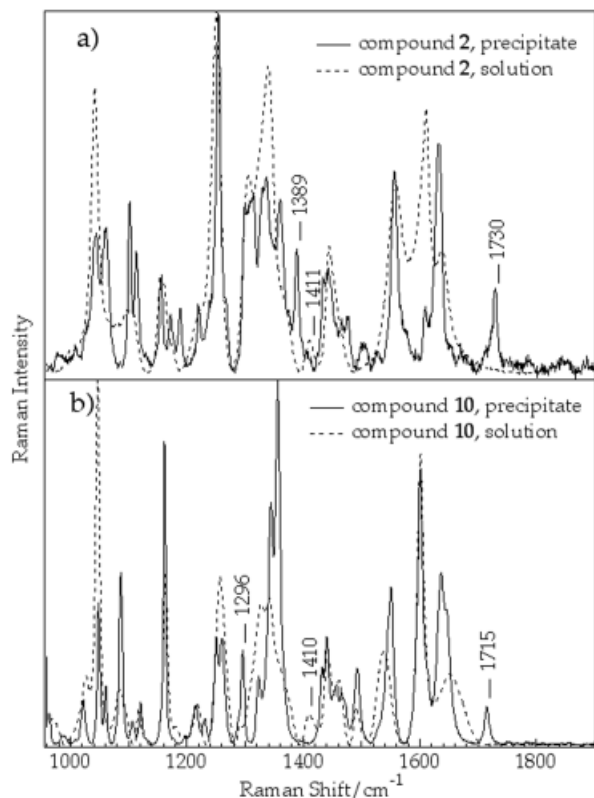


**Figure 3.** The Raman spectra of (---) a 10 mg/mL solution of compounds (a) **1** and (b) **2** at pH 7.4 compared to the Raman spectra of (—) its precipitate form. Only the significant Raman bands are marked.

spectra (Fig. 4). As discussed below, the observed changes are then best interpreted as arising from a mixture of protonated–ionized species whose relative concentrations are pH dependent. For compounds **1**, **2**, and **4** the relative intensity of the peaks at about 1220 and 1300  $\text{cm}^{-1}$  increased while that of the peak at about 1340  $\text{cm}^{-1}$  decreased. A similar trend can be observed in the Raman spectra of compound **8**, except that the frequencies of the peaks involved are at 1196, 1270, and 1344  $\text{cm}^{-1}$  and that the intensity changes were less obvious. These bands disappeared upon deuteration (Fig. 2). After deuteration the only peaks remaining in this region of the Raman spectra are the about 1250 and 1312  $\text{cm}^{-1}$  bands (Figs. 1 and 2). Deuteration of monosubstituted phenolic compounds yields very similar results in that bands previously appearing in this region of the Raman spectra of the undeuterated samples are shifted to another frequency.<sup>39</sup> Moreover, none of the Raman bands for the compounds with a ring-methoxy group (compounds **5** and **10**,

data not shown) exhibited any variation with the pH. Also evident from the Raman spectra of compounds **1**, **2**, and **4** at high pH is the loss of the peak resolution in the 1440–1650  $\text{cm}^{-1}$  regions. Taken together, the results suggest that these vibrational modes originate from the ring-OH bond and/or are due to the perturbation exerted by the hydroxide ion ( $\text{OH}^-$ ) on the ring modes appearing in this region. In a study on phenols, the bands at about 1340 and 1220  $\text{cm}^{-1}$  were assigned to an —OH deformation mode with some ring character. For compound **8** these modes are also affected, but the results are the opposite: the peaks in the 1440–1650  $\text{cm}^{-1}$  regions become more resolved. Although the changes in this region may be attributed to a perturbation of the amide group, this was not the case because, as pointed out above, no apparent changes are observed from the spectra of compounds **5** and **10**.

Alongside the Raman measurements, titration experiments were carried out to determine the apparent  $\text{p}K_a$  of the ring-hydroxy group (Table I). The solution  $\text{p}K_a$  of this group is around 8.5; therefore, increasing the pH to 10 causes the deprotonation of this ring-hydroxy group. Taken together with the Raman results, it is now possible to assign the changes in the intensities (e.g., of the peaks at about 1300 and 1340  $\text{cm}^{-1}$  for compound **2**) as an indicator of the change in the ionization state of the ring-hydroxy group. For example, the intensity ratio ( $I_{1300}/I_{1340}$ ) of the peaks at about 1300 and 1340  $\text{cm}^{-1}$  is 0.7 for compound **2** at pH 7.4 while at pH 10 the ratio is 5. Compound **2** is 90% protonated at pH 7.4 and is completely deprotonated at pH 10. This relationship is useful in the ensuing discussion.

Most of the other identified bands, especially the bands at about 1042, 1159, and 1600  $\text{cm}^{-1}$ , are probably due to various ring modes. Like many of the ring modes in substituted or unsubstituted benzene,<sup>22,23,40,41</sup> the bands at about 1042, 1159, and 1600  $\text{cm}^{-1}$  are not very sensitive to changes in the experimental conditions.

### Raman Spectra at High and Low Concentrations

Table I shows that the apparent hydroxyl  $\text{p}K_a$  values of compounds **2** and **4** increase with the concentration while those of compounds **1**, **8**, and **9** are not affected. As a consequence of the hydroxyl  $\text{p}K_a$  changing with the concentration, the ionization state of the ring-hydroxy group changes. With the pH of the solutions held constant, increasing the concentration should change

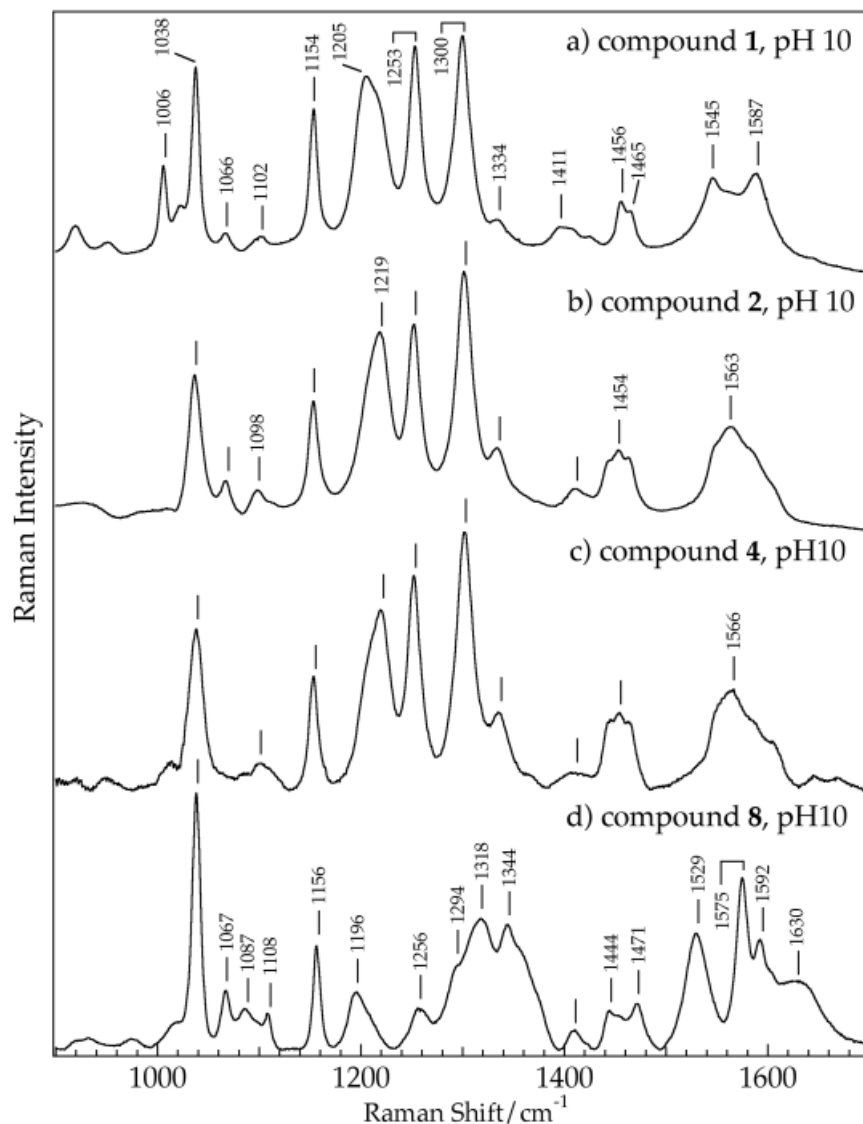


**Figure 4.** Raman spectra of a 10 mg/mL solution of compounds **1** (spectrum a), **2** (spectrum b), **4** (spectrum c), and **8** (spectrum d) at (—) pH 10 compared to that at (---) pH 7.4. The Raman bands that shift by less than 2 cm<sup>-1</sup> relative to the spectra above it are marked but not labeled.

the ratio between the deprotonated and protonated species. Indeed, Figure 5 shows that the  $I_{1300}/I_{1340}$  ratio (the 1300 and 1340 cm<sup>-1</sup> bands being marker bands for the high and low pH forms, respectively) increases with concentration and that the concentration dependence of the  $I_{1300}/I_{1340}$  is smaller for compound **1** than for compounds **2** or **4**. This is because the  $pK_a$  of the ring-hydroxy group of compound **1** is less sensitive to changes in the concentration. In order to rule out or minimize the effect of the pH on the

Raman difference spectra shown below, the pHs of the high and low concentration solutions are adjusted to insure that the parent spectra comprising the difference spectra will have the same  $I_{1300}/I_{1340}$ . In addition, the pH is adjusted (i.e., pH < 8.5 or so) to insure that there is more of the low pH form in the system.

A comparison of the Raman spectra of the compounds at high and low concentrations (Fig. 6) shows subtle differences. To amplify the difference, a Raman difference spectrum is obtained by

**Table I.** Effect of Concentration on  $pK_a$  of Ring-Hydroxy Group and Raman Spectra of Compounds

Compound	$pK_a$ at <sup>a</sup>		Intensity of Raman Difference Bands (% of Parent Peak)				
	10 mg/mL	100 mg/mL	Ring Band	Ring-O Stretch	Ring Band	Ring Band	Amide I Band
1	$8.3 \pm 0.2$	$8.3 \pm 0.2$		22 (1239)	18 (1451)		
2	$8.4 \pm 0.2$	$8.8 \pm 0.2$		10 (1244)	10 (1436)		12 (1644) <sup>b</sup>
				36 (1242)	31 (1437)		19 (1642) <sup>c</sup>
3	$8.4 \pm 0.2$	ND			ND		
4	$8.4 \pm 0.2$	$9.3 \pm 0.2$		18 (1243)	36 (1436)		76 (1645) <sup>d</sup>
5	NA	NA		44 (1243)	35 (1436)		
7	NA	NA	23 (1159)		47 (1437)	24 (1604)	
8	$9.0 \pm 0.2$	$9.0 \pm 0.2$		40 (1245)	24 (1439)		5 (1663)
9	$9.2 \pm 0.2$	$9.2 \pm 0.2$			ND		
10	NA	NA	15 (1253)	33 (1438)			55 (1670)

ND, Not determined, due to some experimental limitations; NA, Not applicable; these compounds do not have a ring-hydroxy group. The numbers in parentheses are the positions of the peaks in terms of frequency ( $\text{cm}^{-1}$ ). Except when specified the difference spectra were obtained from the spectra of 100 and 10 mg/mL solutions.

<sup>a</sup> The uncertainty in the  $pK_a$  represents the accuracy of the instrument.

<sup>b</sup> Raman difference spectra between the Raman spectra of 50 and 10 mg/mL solutions.

<sup>c</sup> Raman difference spectra between the Raman spectra of 150 and 5 mg/mL solutions.

<sup>d</sup> Raman difference spectra between the Raman spectra of 90 and 10 mg/mL solutions.

subtracting the Raman spectra of the compounds at low concentration from the high concentration spectra. The Raman difference spectrum for compound **2** (Fig. 6) reveals a very prominent band that has a positive and negative feature at about  $1244$  and  $1268 \text{ cm}^{-1}$ , respectively. For simplicity, this band is henceforth called the  $1244 \text{ cm}^{-1}$

band. (All difference bands will be referred to by their positive band.) Neither the parent spectra nor the spectra of the compound in other solvents exhibit a band at this position. The same is true with the Raman spectra of the precipitate form. As such, the  $1244 \text{ cm}^{-1}$  band in the difference spectrum can be taken as a marker band for self-

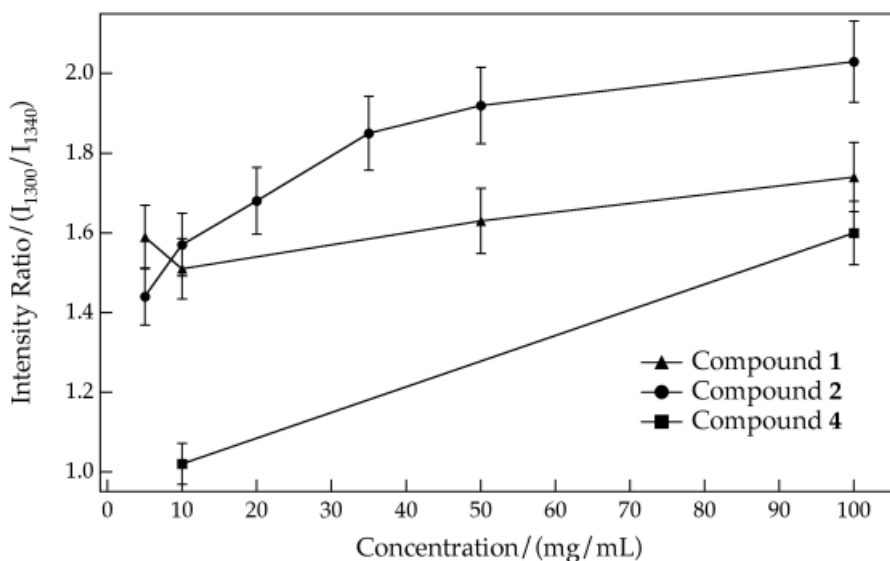


**Figure 5.** The variations of the intensity ratio ( $I_{1300}/I_{1340}$ ) with increasing concentration of compounds **1**, **2**, and **4**. The error bars represent an assumed 5% error in the determination.

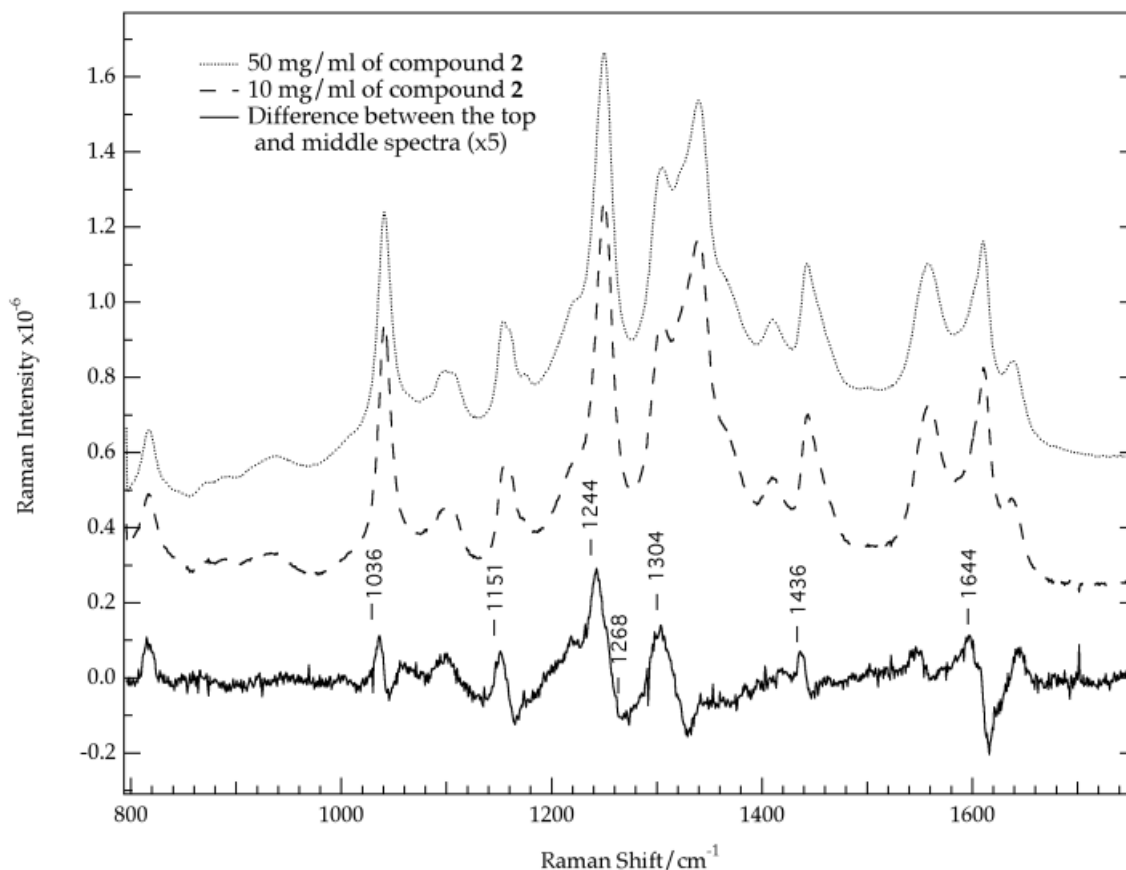


**Figure 6.** (—) The Raman difference spectrum between the ( $\cdots$ ) high and ( $---$ ) low concentration spectra of compound **2**. The lowermost trace represents a blown-up picture of the Raman difference spectrum.

association. There are other bands evident from the Raman difference spectrum of compound **2**, among which are the bands at 1305, 1436, and 1644  $\text{cm}^{-1}$  (Fig. 6). The first difference band is due to a shift in the pH sensitive band at 1304  $\text{cm}^{-1}$ ; the second one can be attributed to a shift in the ring mode at 1444  $\text{cm}^{-1}$ ; and the third one is due to a slight shift in the amide I band (Fig. 1). Table I summarizes some of the prominent Raman difference bands from the spectra of the other compounds studied. The 1240  $\text{cm}^{-1}$  difference band is consistently present among the Raman difference spectra of the compounds exhibiting a 1250  $\text{cm}^{-1}$  band in their parent spectra, (i.e., compounds **1**, **2**, **4**, **5**, **8**, and **10**). It is also evident from the Raman difference spectra of compound **7**, in which the parent spectra do not have an about 1250  $\text{cm}^{-1}$  band, that there are other bands that shifted with the increase in concentration. For this compound the bands that appear at 1159, 1437, and 1604  $\text{cm}^{-1}$  may also be associated with the formation of the self-associate.

To get a sense of how strong the difference bands are, which result from the high and low concentration spectra, the ratio between the intensity of the difference band at 1240  $\text{cm}^{-1}$  and the intensity of the about 1250  $\text{cm}^{-1}$  band in the parent peak were obtained. For compound **2** the difference spectrum between 50 and 10 mg/mL solutions' spectra exhibited a 1240  $\text{cm}^{-1}$  peak that is about 10% of the parent peak. The percentage increased to 36% when the difference between 150 and 5 mg/mL solutions' spectra was taken. This is in agreement with earlier studies that pointed out that compound **2** has already begun to self-associate, even at 10 mg/mL. Turning to the amide I band, the intensity of the difference band, expressed as a percentage of the parent peak at about 1640  $\text{cm}^{-1}$ , varies without any particular trend, which is consistent with the structure of the compounds (Table I). Nonetheless, it is evident that aggregation alters the position of the amide I band (Table I). Interestingly, because the other difference bands (e.g., the one at about 1240

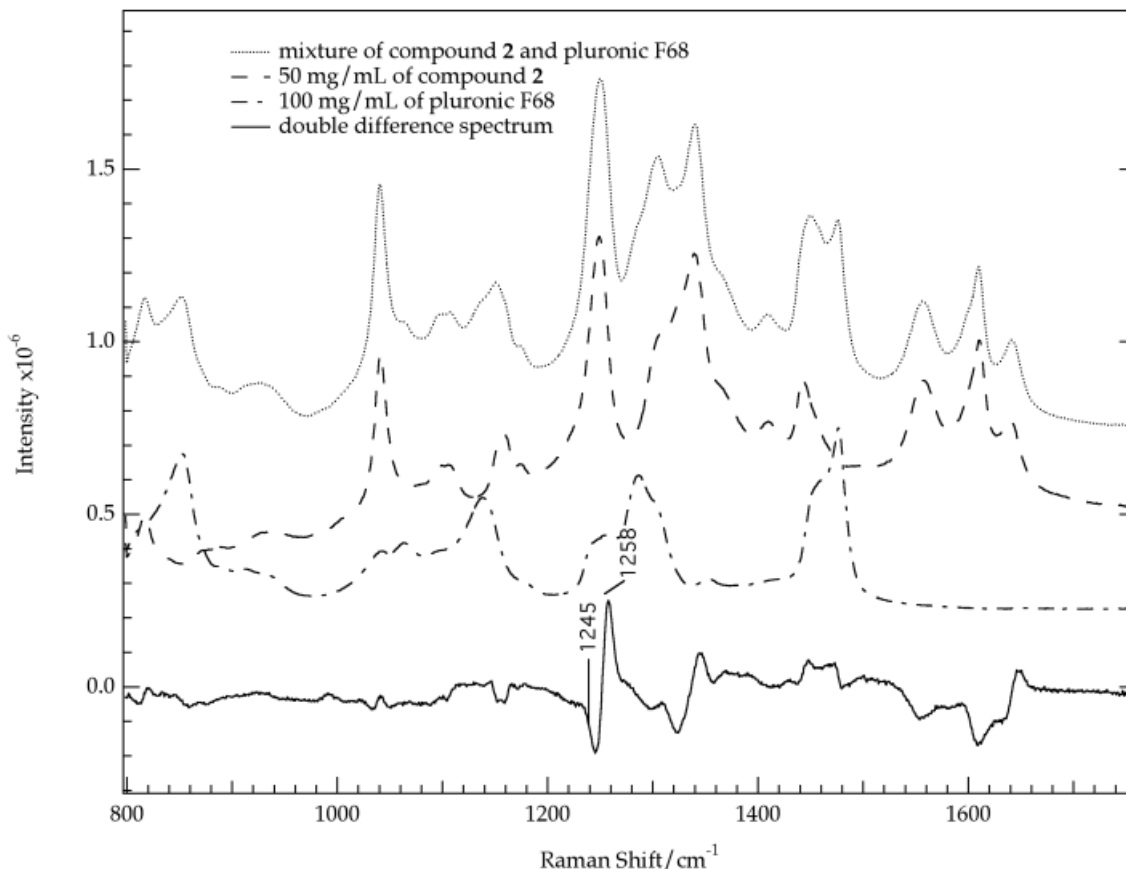


**Figure 7.** (—) The Raman double difference spectrum between the spectra of compound **2** (50 mg/mL) in the (···) presence or (---) absence of an excipient, pluronic F68 (100 mg/mL). (— · —) The spectrum of pluronic F68 in solution by itself is also shown. All solutions are buffered to pH 7.4. The lowermost trace represents a blown-up picture of the Raman double difference spectrum.

$\text{cm}^{-1}$ ) originate from bands earlier identified as coming from a ring mode (aryl-O stretch), aggregation must involve the ring moiety.

In the presence of excipients like propylene glycol, poly(vinyl pyrrolidone), and pluronic F68, which are known to break up self-association, the marker band at  $1240 \text{ cm}^{-1}$  is altered. Figure 7 presents the spectra of compound **2** (50 mg/mL), pluronic F68 (100 mg/mL), and a mixture containing both and the double difference spectrum. The double difference spectrum is obtained by subtracting the spectra of compound **2** and pluronic F68 from the spectrum of the mixture. The  $1250 \text{ cm}^{-1}$  peak in the parent spectra is upshifted in the presence of pluronic F68. In order to rule out that this change is due to variations in the ionic strength of the solution, a double difference spectrum was obtained in the presence of salts like sodium chloride or sodium sulfate (data not

shown). The results show that the upshift of the about  $1250 \text{ cm}^{-1}$  band can only be due to changes in the state of self-association and not to changes in the ionic strength of the solution.

### NMR Spectra of Compounds

Figure 8 shows the 1-D NMR spectra of compound **2** at 100 mg/mL (Fig. 8, spectrum a) and 10 mg/mL (Fig. 8, spectrum b) concentrations in a 90%  $\text{H}_2\text{O}/10\% \text{D}_2\text{O}$  mixture. The resonance down field at 8 ppm in the spectra is due to the NH proton while the four resonances between 6 and 8 ppm are due to the four CH ring protons. The resonances between 1 and 4 ppm are due to aliphatic chain protons. Specifically, the resonance at about 3.3 ppm is assigned to the  $\text{CH}_2$  group next to the amide, and the resonance at about 2.1 ppm is assigned to the  $\text{CH}_2$  group next to the

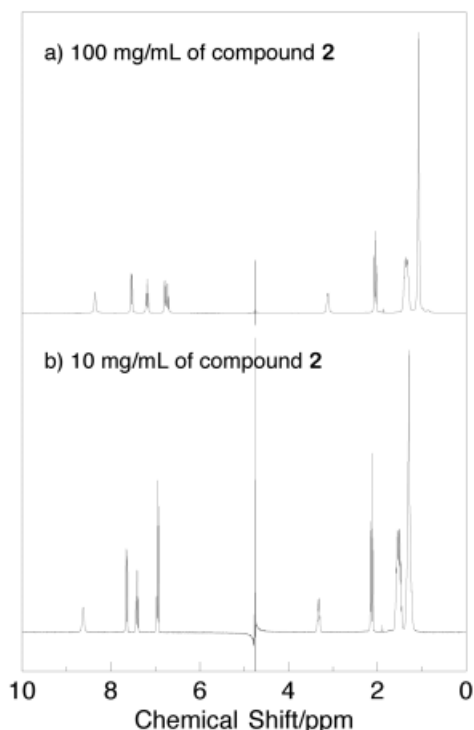


**Figure 8.** The NMR spectra of compound **2** at 100 mg/mL (spectrum a) and 10 mg/mL (spectrum b) in 90% H<sub>2</sub>O/10% D<sub>2</sub>O with 50 mM phosphate buffer at pH 7.4. The water peak at about 4.7 ppm was suppressed by the Watergate technique.

carboxylate. The spike at about 4.7 ppm is due to incomplete suppression of the solvent. The two spectra in Figure 8 appear quite similar, except for a few subtle differences. The concentration increase of compound **2** leads to a 2-Hz (full width at half-height) narrowing of the NH linewidth and about a 0.5-Hz broadening of several CH resonances from both the ring and the aliphatic chain.

The NMR spectra of compound **10** are shown at concentrations of 100 mg/mL (Fig. 9, spectrum a) and 10 mg/mL (Fig. 9, spectrum b) in 90% H<sub>2</sub>O/10% D<sub>2</sub>O. In these spectra the assignments are similar to that of compound **2**, except the sharp resonance at 3.9 ppm is assigned to the CH<sub>3</sub> group of the ring and the resonance at 2.4 ppm is from the CH<sub>2</sub> group next to the amide. Figure 9 shows that a substantial sharpening of the NH resonance occurs when the concentration is increased from about 50 Hz at 10 mg/mL to about 15 Hz at 100 mg/mL. In contrast to compound **2**, no detectable change in the linewidth of the CH resonance is observed.

It is well known that the NH resonance line-

width is normally governed by the rate of proton exchange while that of the CH is governed by the molecular tumbling rate, or correlation time ( $\tau_c$ ). Thus, it is possible to propose a physical picture that is consistent with the concentration dependence of the linewidth changes in the NMR spectra of compounds **2** and **10**. For compound **10** the much sharper NH resonance at a high concentration indicates that NH exchanges more slowly with solvent, suggesting that the NH group is somewhat protected from the solvent at a high concentration. For compound **2** the NH proton exchange rate is already low (relative to that in compound **10**) at 10 mg/mL; hence, there is only a relatively small sharpening of the NH resonance when the concentration is further increased. Furthermore, the small broadening of the CH resonance in compound **2** at a higher concentration indicates a decrease in the tumbling motion of the related protons. Thus, the concentration dependence of both the NH and CH resonance linewidths of compound **2** suggests increased self-association at higher concentrations.

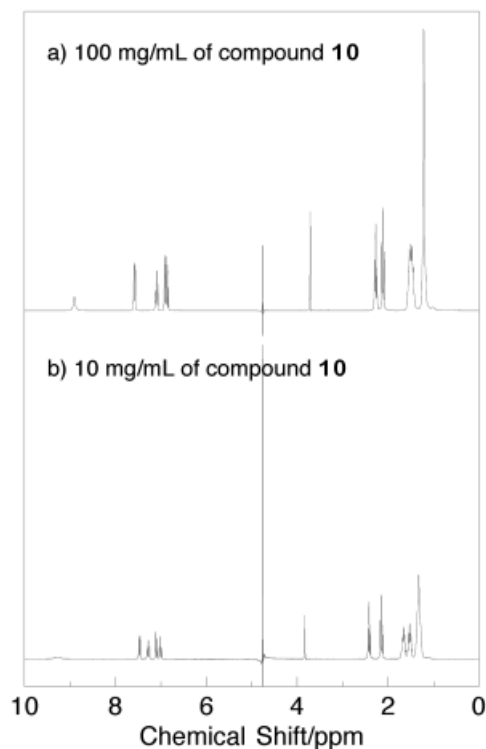


**Figure 9.** The NMR spectra of compound **10** at 100 mg/mL (spectrum a) and 10 mg/mL (spectrum b) in 90% H<sub>2</sub>O/10% D<sub>2</sub>O with 50 mM phosphate buffer at pH 7.4. The water peak at about 4.7 ppm was suppressed by the Watergate technique.

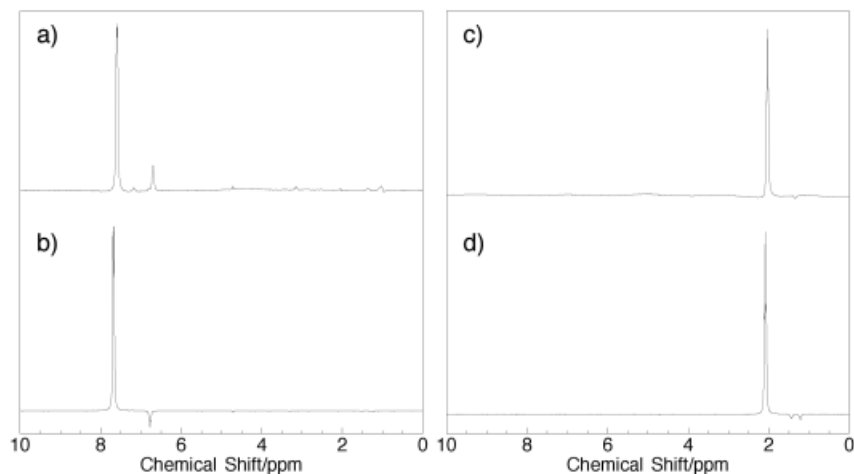


**Figure 10.** The results of a 1-D selective NOESY experiment on compound **4** at concentrations of 50 and 10 mg/mL at pH 8 in D<sub>2</sub>O. The results are shown from the solutions at 50 mg/mL (spectrum a) and 10 mg/mL (spectrum b) when one of the ring protons was on resonance with the selective pulse. The results are also shown from the solutions at 50 mg/mL (spectrum c) and 10 mg/mL (spectrum d) when two of the chain protons nearest the carboxyl group was on resonance with the selective pulse. The mixing time for all measurements is set to 400 ms.

In order to determine if the tumbling rate decrease is uniform along the molecule when the concentration is increased, 1-D selective NOESY measurements were performed on compound **4** at two different concentrations. The standard 1-D NMR spectrum of this compound is almost identical to compound **2**, because the protons of the two additional CH<sub>2</sub> groups contribute only to a resonance at 1.3 ppm. The selective pulse is either in resonance with either one of the ring protons (Fig. 10, spectra a and b at 50 and 10 mg/mL, respectively) or the two chain protons next to the carboxylic group (Fig. 10, spectra c and d at 50 and 10 mg/mL, respectively). In these spectra, the major peak is the selectively inverted one and the small peak(s) near the major one is the NOEs from the nearby proton(s). The results show that at 10 mg/mL the NOEs between either the ring protons (Fig. 10, spectrum b) or the tail protons (Fig. 10, spectrum d) are positive (opposite to the selected peak), indicating that the tumbling rate of the entire molecule is fast and  $\omega\tau_c \ll 1$  for all protons, where  $\omega$  is the Larmor frequency of the proton. However, when the concentration is increased to 50 mg/mL, the NOEs between the ring protons become negative (on the same side of the selected peak, Fig. 10, spectrum a). This suggests that the tumbling rate of the ring is significantly slowed and the  $\omega\tau_c$  becomes much larger than 1. In contrast, the NOE between aliphatic protons

remains positive, even though its intensity is considerably decreased. Such a result suggests that the tumbling motion of the tail is not significantly hindered with increasing concentration. Thus, the NMR results are consistent with the Raman observation that the major interaction among delivery agents may be localized to the ring portion of the delivery agent.

## DISCUSSION

This work is focused on developing an understanding of the solution structures of molecules that have shown promise as drug delivery agents, which are based on amidated acids. Vibrational and NMR spectroscopies were both used to characterize their solution properties. Studies were performed at high and low concentrations to investigate at what point these molecules self-associate and which interactions are responsible for their self-association and to characterize the structures of the monomer and the self-associated complex.

Most of the major bands in the vibrational spectra of the delivery agents arise from the ring moiety. One ring band at about 1250 cm<sup>-1</sup>, assigned to the aryl-O stretch, is of special interest because it downshifts when the delivery agents self-associate. The Raman spectra of those molecules whose ring moiety contain a hydroxyl moiety change drastically

upon ionization of this group. In particular, we used the relative intensity at 1300 versus 1340  $\text{cm}^{-1}$  to indicate the relative proportion of unprotonated hydroxyl. Finally, a clear set of marker bands showing the ionization state of the end group carboxyl are at 1410 and 1715  $\text{cm}^{-1}$  for ionized and protonated, respectively.

At physiological pH the —NH bond and the ring-hydroxyl of compounds **1**, **2**, **3**, **4**, **6**, **8**, and **9** both remain protonated while the carboxylic is ionized in the monomers. On the other hand, the carboxylic end of the molecule is protonated in the precipitate. In essence the —NH and —OH acidic hydrogens in the structure of the compounds are available to form hydrogen bonds with electronegative groups such as water, intermolecular contacts with themselves in self-associated complexes, or polar groups of various drugs. It is clear that the ionized carboxylate is important to keep these compounds, which generally contain substantial hydrophobicity with regard to the alkane groups and the ring systems, in aqueous solution. This class of compounds is quite insoluble at pH values below about 7.5. Because the  $\text{p}K_a$  of their carboxyl groups must be close to that of acetic acid (about 4.2), the low solubility near neutral pH suggests that the very small amounts of protonated species that exist in solution at pH 7.5 have a strong tendency to self-associate and in most instances drop out of solution in a runaway reaction. The delivery agent/drug complex must be stable and “soluble” in both the aqueous solution and the hydrophobic environment of the interior of the lipid bilayer of the cellular membrane. The observations on the delicate balance of the solubility of these delivery agents suggest the possibility that they can protonate in their self-associates and/or in their close interaction with drugs like heparin. The barrier to the diffusion of the uncharged (protonated) drug–delivery agent complexes through the interior of the lipid bilayer should be significantly lower than that of the charged (ionized) drug–delivery agent complexes.

Self-association of these compounds at neutral pH occurs at higher concentrations. Although there were no systematic studies performed, it is clear that there is significant self-association occurring at concentrations as low as 8 mg/mL for some compounds (i.e., compound **2**). The self-associated complex is characterized by the following structural attributes. In our subsequent article careful studies of compound **2** showed that the carboxyl group is predominantly, but not exclusively, ionized. Hence, in general, this group is

likely distributed in the self-associate to not be in close proximity to another carboxylate due to charge–charge repulsion of the end group. There is a ring–ring interaction as indicated by the downshift of the aryl-O stretch band at about 1250  $\text{cm}^{-1}$ . Various studies were performed on the nature of the interactions of aromatic ring compounds, and several conformations were considered. Two of the many possibilities are most probable. One involves the formation of a hydrogen bond between a ring proton (or a proton of a proton donor like —OH) and the  $\pi$  electron system of the aromatic ring, forming a T-shaped geometry. Calculations show this is energetically stable and this motif was observed in the structures of proteins, for example. Another configuration that is possible is a structure whereby the two rings are parallel and sandwiched together but displaced from each other (parallel displaced). It is very unlikely that the T-shaped structure is involved in the intermolecular action observed for the compounds studied here. First, the degree of self-association grows with increasing concentration and there is little geometry that can support a T-shaped configuration. Second, the ring hydroxyl of some of the compounds (e.g., compound **1**) does not change its  $\text{p}K_a$  upon self-association (Table I), which would be expected if this group formed an intermolecular hydrogen bond with the  $\pi$  electron system of another ring. For some of the compounds there are downshifts in the C=O stretch mode of the amide group (Table I). Such shifts were observed in many systems and are brought about by the formation of intermolecular hydrogen bonds with either the amide C=O group and/or the —NH moiety.<sup>24</sup> For example, a proton donor hydrogen bonding to C=O polarizes the C=O bond, reducing its bond order and concomitantly its stretch frequency. In agreement with these observations based on the vibrational spectroscopy, the NMR results show that the —NH proton exchanges more slowly with solvent in the self-associate in solution than for isolated molecules and the ring tumbling rate is reduced. On the other hand, the tumbling motion of the tail is not significantly hindered with increasing concentration. Thus, the NMR results are consistent with the Raman observation that the major interaction among delivery agents appears to be localized to the ring portion.

This publication was developed under the auspices of the City University of New York CAT in Ultrafast Photonic Materials and Applications, a New York State Center for Advanced Technology

supported by the New York State Science and Technology Foundation.

## REFERENCES

1. Leone-Bay, A.; Santiago, N.; Achan, D.; Chaudhary, K.; DeMorin, F.; Falzarano, L.; Haas, S.; Kalbag, S.; Kaplan, D.; Leipold, H.; Lercara, C.; O'Toole, D.; Rivera, T.; Rosado, C.; Sarubbi, D.; Vuocolo, E.; Wang, N.; Milstein, S.; Baughman, R. A. *J Med Chem* 1995, 38, 4263–4269.
2. Leone-Bay, A.; Ho, K.-K.; Agarwal, R.; Baughman, R. A.; Chaudhary, K.; DeMorin, F.; Genoble, L.; McInnes, C.; Lercara, C.; Millstein, S.; O'Toole, D.; Sarubbi, D.; Variano, B.; Paton, D. R. *J Med Chem* 1996, 39, 2571–2578.
3. DalPozzo, A.; Acquasaliente, M.; Geron, M. R. *Thromb Res* 1989, 56, 119–124.
4. Gonze, M. D.; Manord, J. D.; Leone-Bay, A.; Baughman, R. A.; Garrard, C. L.; Sternbergh III, W. C.; Money, S. R. *Am J Surg* 1998, 176, 176–178.
5. Baughman, R. A.; Kapoor, S. C.; Agarwal, R. K.; Kisicki, J.; Catella-Lawson, F.; Fitzgerald, G. A. *Circulation* 1998, 98, 1610–1615.
6. Leone-Bay, A.; Leipold, H.; Agarwal, R.; Rivera, T.; Baughman, R. A. *Drugs Future* 1997, 22, 885–891.
7. Leone-Bay, A.; Paton, D. R.; Variano, B.; Leipold, H.; Rivera, T.; Miura-Fraboni, J.; Baughman, R. A.; Santiago, N. *J Controlled Release* 1998, 50, 41–49.
8. Leone-Bay, A.; Paton, D. R.; Freeman, J.; Lercara, C.; O'Toole, D.; Gschneider, D.; Wang, E.; Harris, E.; Rosado, C.; Rivera, T.; DeVincent, A.; Tai, M.; Mercogliano, F.; Agarwal, R.; Leipold, H.; Baughman, R. A. *J Med Chem* 1998, 41, 1163–1171.
9. Brayden, D.; Creed, E.; O'Connell, A.; Leipold, H.; Agarwal, R.; Leone-Bay, A. *Pharm Res* 1997, 14, 1772–1779.
10. Leone-Bay, A.; Leipold, H. R.; Paton, D. R.; Milstein, S. J.; Baughman, R. A. *D N P* 1996, 9, 586–591.
11. Haas, S.; Miura-Fraboni, J.; Zavala, F.; Murata, K.; Leone-Bay, A.; Santiago, N. *Vaccine* 1996, 14, 785–791.
12. Rivera, T.; Leone-Bay, A.; Paton, D. R.; Leipold, H. R.; Baughman, R. A. *Pharm Res* 1997, 14, 1830–1834.
13. Carey, P. R. *Biochemical Applications of Raman and Resonance Raman Spectroscopy*; Academic: New York, 1982.
14. Spiro, T. G., Ed. *Biological Applications of Raman Spectroscopy*, Vol. 1; Wiley: New York, 1987.
15. Spiro, T. G., Ed. *Biological Applications of Raman Spectroscopy*, Vol. 2; Wiley: New York, 1987.
16. Spiro, T. G., Ed. *Biological Applications of Raman Spectroscopy*, Vol. 3; Wiley: New York, 1988.
17. Deng, H.; Callender, R. *Comments Mol Cell Biophys* 1993, 8, 137–154.
18. Callender, R.; Deng, H. *Annu Rev Biophys Biomol Struct* 1994, 23, 215–245.
19. Callender, R.; Deng, H.; Gilmanishin, R. *J Raman Spectrosc* 1998, 29, 15–21.
20. Hadzi, D.; Sheppard, N. *Proc R Soc Ser A* 1953, 216, 247–266.
21. Evans, J. C. *Spectrochim Acta* 1960, 16, 1382–1392.
22. Colthup, N. B.; Daly, L. H.; Wiberley, S. E. *Introduction to Infrared and Raman Spectroscopy*; Academic: San Diego, CA, 1990.
23. Lin-Vien, D.; Colthup, N. B.; Fateley, W. G.; Grasselli, J. G. *The Handbook of Infrared and Raman Characteristic Frequencies of Organic Molecules*; Academic: San Diego, CA, 1991.
24. Deng, H.; Schindler, J. F.; Berst, K. B.; Plapp, B. V.; Callender, R. *Biochemistry* 1998, 37, 14267–14278.
25. Carey, P. R.; Tonge, P. *J Acc Chem Res* 1995, 28, 8–15.
26. Doran, J. D.; Carey, P. R. *Biochemistry* 1996, 35, 12495–12502.
27. Ray, W. J.; Burgner, J. W.; Post, C. B. *Biochemistry* 1990, 29, 2770–2778.
28. Chen, Y.-Q.; Kraut, J.; Callender, R. *Biophys J* 1997, 72, 936–941.
29. Deng, H.; Chan, A. Y.; Bagdassarian, C. K.; Estupinan, B.; Ganem, B.; Callender, R. H.; Schramm, V. L. *Biochemistry* 1996, 35, 6037–6047.
30. Gilmanishin, R.; Van Beek, J.; Callender, R. *J Phys Chem* 1996, 100, 16754–16760.
31. Gilmanishin, R.; Williams, S.; Callender, R. H.; Woodruff, W.; Dyer, R. B. *Proc Natl Acad Sci USA* 1997, 94, 3709–3713.
32. Joesten, M.; Schaad, L. J. *Hydrogen Bonding*; Marcel Dekker: New York, 1974.
33. Thijs, R.; Zeegers-Huyskens, T. *Spectrochim Acta* 1984, 40A, 307–313.
34. Latajka, Z.; Scheiner, S. *Chem Phys Lett* 1990, 174, 179–184.
35. Desamero, R.; Cheng, H.; Cahill, S.; Girvin, M.; Callender, R.; Rath, P.; Variano, B.; Smart, J. *Biopolym Biospectrosc*, submitted.
36. Piotto, M.; Saudek, M.; Sklenar, V. *J Biomol NMR* 1992, 2, 661–665.
37. Stott, K.; Stonehouse, J.; Keeler, J.; Hwang, T.-L.; Shaka, A. J. *J Am Chem Soc* 1995, 117, 4199–4200.
38. Miyazawa, T.; Shimanouchi, T.; Mizushima, S. *J Chem Phys* 1955, 24, 408–418.
39. Green, J. H. S.; Harrison, D. J.; Kynaston, W. *Spectrochim Acta* 1971, 27A, 2199–2217.
40. Katritzky, A. R.; Lagowski, J. M. *J Chem Soc Lond* 1958, 4155–4162.
41. Katritzky, A. R.; Coats, N. A. *J Chem Soc Lond* 1959, 2062–2066.
42. Agarwal, R.; Chaudhary, K.; Barantsevich, E.; Harris, E.; Paton, D.; Ho, K.-K.; Baughman, R. Abstract presented at the Meeting of the American Association of Pharmaceutical Science, 1996.
43. Hobza, P.; Selzle, H.; Schlag, E. *Chem Rev* 1994, 94, 1767–1785.